JGP Journal of General Physiology

RESEARCH ARTICLE

# Cardiomyopathy mutation (F88L) in troponin T abolishes length dependency of myofilament $Ca^{2+}$ sensitivity

Sherif M. Reda and Murali Chandra

**Recent clinical studies have revealed a new hypertrophic cardiomyopathy–associated mutation (F87L) in the central region of human cardiac troponin T (TnT). However, despite its implication in several incidences of sudden cardiac death in young and old adults, whether F87L is associated with cardiac contractile dysfunction is unknown. Because the central region of TnT is important for modulating the muscle length–mediated recruitment of new force-bearing cross-bridges (XBs), we hypothesize that the F87L mutation causes molecular changes that are linked to the length-dependent activation of cardiac myofilaments. Length-dependent activation is important because it contributes significantly to the Frank–Starling mechanism, which enables the heart to vary stroke volume as a function of changes in venous return. We measured steady-state and dynamic contractile parameters in detergent-skinned guinea pig cardiac muscle fibers reconstituted with recombinant guinea pig wild-type TnT ($TnT_{WT}$) or the guinea pig analogue ($TnT_{F88L}$) of the human mutation at two different sarcomere lengths (SLs): short (1.9 µm) and long (2.3 µm). $TnT_{F88L}$ increases $pCa_{50}$ (−log $[Ca^{2+}]_{free}$ required for half-maximal activation) to a greater extent at short SL than at long SL; for example, $pCa_{50}$ increases by 0.25 pCa units at short SL and 0.17 pCa units at long SL. The greater increase in $pCa_{50}$ at short SL leads to the abolishment of the SL-dependent increase in myofilament $Ca^{2+}$ sensitivity ($\Delta pCa_{50}$) in $TnT_{F88L}$ fibers, $\Delta pCa_{50}$ being 0.10 units in $TnT_{WT}$ fibers but only 0.02 units in $TnT_{F88L}$ fibers. Furthermore, at short SL, $TnT_{F88L}$ attenuates the negative impact of strained XBs on force-bearing XBs and augments the magnitude of muscle length–mediated recruitment of new force-bearing XBs. Our findings suggest that the $TnT_{F88L}$-mediated effects on cardiac thin filaments may lead to a negative impact on the Frank–Starling mechanism.**

## Introduction

Hypertrophic cardiomyopathy (HCM) mutations in the central region (CR; residues 80–180) of cardiac troponin T (TnT) are not well tolerated, perhaps because of their negative impact on thin filament cooperativity and length-dependent activation of cardiac myofilaments. Previous work from our laboratory has demonstrated that the structural integrity of CR is important for thin filament cooperativity and length-dependent activation of cardiac myofilaments (Ford et al., 2012; Gollapudi and Chandra, 2016a,b). Recent studies have suggested that impairment of length-dependent activation may be one of the primary mechanisms by which HCM mutations lead to altered cardiac phenotype and deleterious complications associated with HCM (Sequeira et al., 2013). Clinical data have recently discovered a mutation in the CR of human TnT (F87L) that is associated with HCM and high incidences of sudden cardiac death in young and old adults (Gimeno et al., 2009). However, cardiac contractile dysfunction associated with the F87L mutation in human TnT is unknown.

Mutation-mediated impairment of length-dependent activation may have significant implications for intact heart function because length-dependent activation underlies the molecular basis for the Frank–Starling mechanism, which describes the ability of the heart to regulate cardiac output in response to beat-to-beat variations in end-diastolic volume (Allen and Kentish, 1985; Plotnick et al., 1986; Holubarsch et al., 1996; Konhilas et al., 2002a; Nowak et al., 2007; Abraham et al., 2016). Indeed, impairment of length-dependent activation has been observed in several cases of cardiomyopathies (van Dijk et al., 2012) and failing human hearts (Schwinger et al., 1994; Sequeira et al., 2013). At the myofilament level, cardiac muscle exhibits pronounced length-dependent activation, whereby an increase in sarcomere length (SL) augments myofilament $Ca^{2+}$ sensitivity (Allen and

Department of Integrative Physiology and Neuroscience, Washington State University, Pullman, WA.

Correspondence to Murali Chandra: murali@vetmed.wsu.edu.

Kentish, 1985; Wang and Fuchs, 1994; Konhilas et al., 2002a), leading to the recruitment of force-bearing cross-bridges (XBs) and an increase in myocardial force production. Such SL-mediated enhancement of myofilament $Ca^{2+}$ sensitivity is regulated by cooperative mechanisms that feed back to activate cardiac thin filaments in response to an increase in SL (Allen and Kentish, 1985; Fitzsimons and Moss, 1998; Moss and Fitzsimons, 2002; Smith et al., 2009). In this context, interventions that increase myofilament $Ca^{2+}$ sensitivity and/or alter XB-based cooperative mechanisms have been shown to alter SL-dependent function in cardiac muscle (Fitzsimons and Moss, 1998; Arteaga et al., 2000; Ford et al., 2012; Kobirumaki-Shimozawa et al., 2014). For example, a previous study has demonstrated that the R92L mutation in the CR of mouse TnT enhances myofilament $Ca^{2+}$ sensitivity but abolishes the SL-mediated increase in myofilament $Ca^{2+}$ sensitivity (Ford et al., 2012). Because thin filament cooperativity and muscle length (ML)-mediated XB recruitment dynamics are significantly modulated by the CR of TnT (Gollapudi et al., 2013), HCM-associated mutations in the CR are expected to have a negative impact on length-dependent activation.

To investigate the effect of F87L on contractile function and whether such effects varied in an SL-dependent manner, recombinant guinea pig wild-type TnT ($TnT_{WT}$) and mutant TnT ($TnT_{F88L}$) were generated and reconstituted into detergent-skinned papillary muscle fibers isolated from guinea pig left ventricles. Guinea pig cardiac tissue was preferred because guinea pigs, like humans (Narolska et al., 2005a,b), predominantly express the β-myosin heavy chain (β-MHC) isoform in the myocardium (van der Velden et al., 1998). MHC isoform becomes an important aspect to consider when assessing the effect of mutations in the CR because the effects of CR on contractile function are modulated differently by α- and β-MHC isoforms (Ford et al., 2012; Gollapudi and Chandra, 2016a,b). For example, R92L in TnT abolishes the length-dependent increase in myofilament $Ca^{2+}$ sensitivity in β-MHC–expressing fibers, but not in α-MHC–expressing fibers, suggesting that the effect of TnT-mediated changes on length-dependent activation depends on the type of MHC isoform (Ford et al., 2012). In addition, muscle fibers expressing β-MHC have been shown to exhibit steeper SL-dependent changes in dynamic contractile parameters (Korte and McDonald, 2007; Ford et al., 2012). Steady-state and dynamic contractile parameters were measured in $TnT_{WT}$ and $TnT_{F88L}$ muscle fibers at two different SLs (1.9 µm and 2.3 µm). Our results demonstrated that $TnT_{F88L}$ abolished the SL-mediated increase in cardiac myofilament $Ca^{2+}$ sensitivity. Moreover, the magnitude of ML-mediated recruitment of XBs ($E_R$) and the negative impact of strained XBs on recruitment of force-bearing XBs ($\gamma$) were altered in an SL-dependent manner.

## Materials and methods

### Animal protocols

8–10-mo-old male Dunkin-Hartley guinea pigs (*Cavia porcellus*) acquired from Charles River were used in this study. All animals were housed in environmentally controlled rooms of an Association for Assessment and Accreditation of Laboratory Animal Care–accredited facility under 12-h light and dark cycles. All animals received proper care and treatment in accordance with the preapproved protocols by Washington State University Institutional Animal Care and Use Committee. The procedures for euthanizing guinea pigs conformed to the recommendations of the American Veterinary Medical Association, as outlined in the Guidelines for the Euthanasia of Animals.

### Expression and purification of recombinant guinea pig cardiac troponin subunits

Recombinant *c-myc*–tagged guinea pig TnT ($TnT_{WT}$ and $TnT_{F88L}$), guinea pig WT troponin I (TnI), and guinea pig WT troponin C (TnC) were generated and cloned into a pSBETa vector (GenScript USA). The inclusion of the *c-myc* tag has been previously shown to have no effect on contractile function (Tardiff et al., 1998; Montgomery et al., 2001; Chandra et al., 2005). Recombinant DNA was transformed and expressed in BL21*DE3 cells (Invitrogen). In brief, $TnT_{WT}$ and $TnT_{F88L}$ were purified by ion-exchange chromatography on a DEAE-Fast Sepharose column (GE Healthcare Biosciences). TnI was purified using a CM Sepharose ion-exchange column, and TnC was purified using a DE-52 column and phenyl Sepharose column. Details on protein purification can be found in the Supplemental materials and methods.

### Reconstitution of recombinant troponin complexes in detergent-skinned guinea pig cardiac muscle fibers

Left ventricular guinea pig papillary muscle fibers were prepared and detergent skinned, as described in the Supplemental materials and methods. Reconstitution of recombinant troponin into cardiac muscle fibers was done as previously described (Chandra et al., 1999; Gollapudi et al., 2012; Mamidi et al., 2013). Recombinant $TnT_{WT}$ or $TnT_{F88L}$ (0.9 mg/ml, wt/vol) and TnI (1.0 mg/ml, wt/vol) were dissolved in an exchange buffer containing the following: 50 mM Tris-HCl, 6 M urea, and 1.0 mM KCl, pH 8.0, at 4°C (buffer 1). To remove high salt and urea, proteins were successively dialyzed against 50 mM Tris-HCl, 4 M urea, and 0.7 M KCl, pH 8.0, at 4°C (buffer 2); 50 mM Tris-HCl, 2 M urea, and 0.5 M KCl, pH 8.0, at 4°C (buffer 3); and 50 mM *N,N*-bis (2-hydroxyethyl)-2-aminoethanesulfonic acid (BES), 200 mM KCl, 10 mM 2,3-butanedione monoxime (BDM), 6.27 mM $MgCl_2$, and 5 mM EGTA, pH 7.0, at 22°C (buffer 4). All buffers included a cocktail of protease inhibitors (0.2 mM PMSF, 2 mM benzamidine-HCl, 1 mM dithiothreitol (DTT), and 0.01% sodium azide). Any undissolved protein in the exchange buffer was removed by centrifugation at 3,000 rpm for 15 min. Detergent-skinned fiber bundles were treated with the exchange buffer containing $TnT_{WT}$ + TnI or $TnT_{F88L}$ + TnI for ∼3 h at room temperature (22°C) with gentle stirring. Muscle fiber bundles were then washed twice (10 min each) with buffer 4 to remove remnants of exchange buffer, followed by overnight incubation at 4°C in high-relaxing solution containing TnC (3.0 mg/ml, wt/vol).

### Measurement of isometric steady-state tension and ATPase activity

Steady-state isometric tension was measured in muscle fibers at various pCa values ($-\log_{10}$ of $[Ca^{2+}]_{free}$), as previously described

(de Tombe and Stienen, 1995; Stienen et al., 1995; Campbell et al., 2004; Gollapudi et al., 2015). The composition of pCa solutions can be found in the Supplemental materials and methods. In brief, muscle fibers were mounted between a motor arm (322C; Aurora Scientific) and a force transducer (AE 801; Sensor One Technologies). SL was set to 1.9 or 2.3 µm in high-relaxing solution using He-Ne laser diffraction technique (de Tombe and Stienen, 1995). Each muscle fiber was exposed to various pCa solutions ranging from 4.3 to 9.0 in a constantly stirred chamber maintained at a temperature of 20°C. Force responses were recorded on a computer at a sampling rate of 1 kHz. Isometric steady-state tension was calculated at each pCa and normalized to maximal tension (tension at pCa 4.3). Normalized steady-state tension was then plotted against respective pCa to construct the pCa–tension relationship. For each muscle fiber, the Hill equation was fitted to the normalized pCa–tension data to estimate two parameters, $pCa_{50}$ and $n_H$, indices of myofilament $Ca^{2+}$ sensitivity and myofilament cooperativity, respectively.

ATPase activity was measured using an enzymatically coupled reaction that couples the breakdown and regeneration of ATP to the oxidation of NADH (de Tombe and Stienen, 1995; Stienen et al., 1995; Chandra et al., 2006). In brief, near-UV light was projected through the measuring chamber, and a beam splitter (50:50) was used to detect wavelengths of 340 nm (sensitive to changes in NADH) and 400 nm (insensitive to changes in NADH). Because the oxidation of NADH is enzymatically coupled to the breakdown and regeneration of ATP, changes in ATPase activity can be estimated from changes in NADH, which is measured by changes in UV absorbance at 340 nm. The UV absorbance signal of NADH was calibrated by multiple injections of 250 pmol ADP into the measuring chamber. Tension cost was derived from the ATPase–tension relationship, as previously described (de Tombe and Stienen, 1995; Chandra et al., 2015).

### Measurement of muscle fiber mechanodynamics

Upon attainment of maximal steady-state activation, the motor arm was commanded to elicit various amplitude stretch/release perturbations (±0.5, ±1.0, ±1.5, and ±2.0% of the initial ML) to the attached muscle fibers (Ford et al., 2010). Each length perturbation was maintained for 5 s, and the corresponding force responses were recorded to highlight three different phases. As described previously (Ford et al., 2010), a nonlinear recruitment-distortion (NLRD) model was fitted to the force response phases to estimate five model parameters: the magnitude of the instantaneous increase in force caused by a sudden increase in ML ($E_D$); the rate by which force drops because of dissipation of strain within bound XBs ($c$); a nonlinear interaction term representing the negative effect of strained XBs on other force-bearing XBs ($\gamma$); the rate by which XBs are recruited into the force-bearing state at the new ML ($b$); and the magnitude of increase in steady-state force caused by recruitment of additional force-bearing XBs at the increased ML ($E_R$). Fig. 1 depicts the length protocol of 2% sudden stretch (Fig. 1 A) and the corresponding force response (Fig. 1 B) from a muscle fiber. Details on the physiological significance of each model parameter can be found in the Supplemental materials and methods.

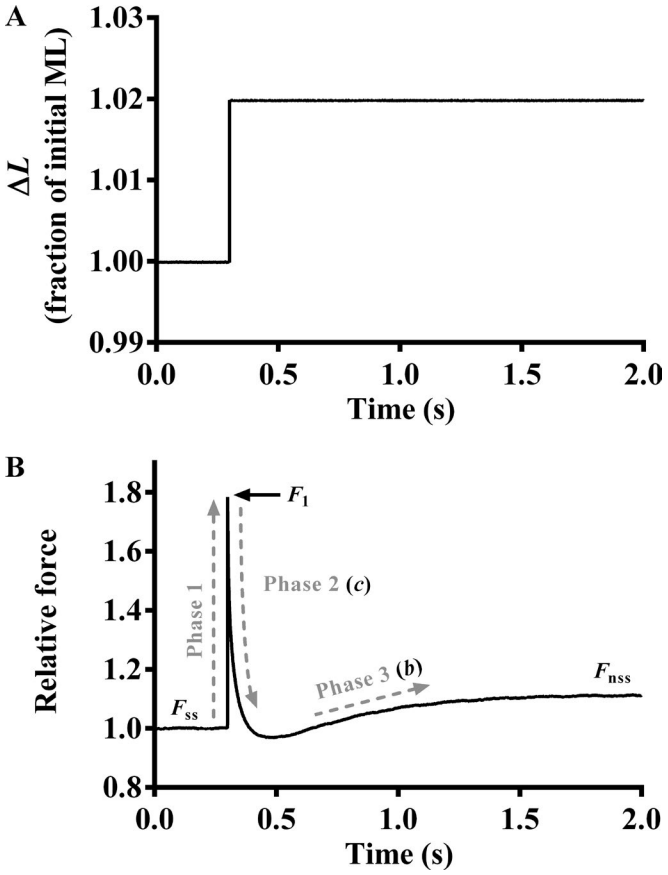


Figure 1. **Representative force response to a sudden 2% stretch. (A)** A representative 2% sudden stretch in ML imposed on a $TnT_{WT}$ muscle fiber at maximal $Ca^{2+}$ activation (pCa 4.3). **(B)** The corresponding force response normalized to the isometric steady-state force ($F_{ss}$) before ML change. The NLRD model was fitted to the family of force responses to steplike changes in ML (±0.5, ±1.0, ±1.5, and ±2.0% of initial ML) to estimate various model parameters (Ford et al., 2010). The different phases (dashed lines) from which the respective parameters were estimated are highlighted. $F_1$, the instantaneous increase in force caused by sudden increase in ML (phase 1); $c$, the rate by which force decays to a minimum point after a sudden stretch in ML (phase 2); $\gamma$, a nonlinear interaction term representing the negative impact of strained XBs on other force-bearing XBs; $b$, the rate of delayed force rise after an increase in ML (phase 3); $F_{nss}$, the new steady-state force corresponding to an increase in ML.

### Rate constant of tension redevelopment

The rate constant of tension redevelopment ($k_{tr}$) was estimated using a modified version of the large slack/restretch maneuver originally designed by Brenner and Eisenberg (1986) and is described in the Supplemental materials and methods.

### Statistical analysis

Our experimental model investigated the effects of two factors, TnT ($TnT_{WT}$ and $TnT_{F88L}$) and SL (1.9 and 2.3 µm). Thus, two-way ANOVA was constructed to analyze the effect of TnT on each contractile parameter at a given SL. A significant TnT–SL interaction effect suggested that the effect of $TnT_{F88L}$ on a given parameter

Table 1. **Effect of $TnT_{F88L}$ on various contractile parameters at short and long SLs**

| Parameter | 1.9 µm | | 2.3 µm | |
|---|---|---|---|---|
| | $TnT_{WT}$ | $TnT_{F88L}$ | $TnT_{WT}$ | $TnT_{F88L}$ |
| Maximal tension ($mN \cdot mm^{-2}$) | 29.72 ± 1.25 | 31.63 ± 1.52[a] | 49.07 ± 1.24 | 48.25 ± 0.93[a] |
| Tension cost ($pmol \cdot mN^{-1} \cdot mm^{-1} \cdot s^{-1}$) | 2.56 ± 0.17 | 2.34 ± 0.11[a] | 1.26 ± 0.06 | 1.32 ± 0.07[a] |
| $c$ ($s^{-1}$) | 12.17 ± 0.42 | 10.98 ± 0.89[a] | 7.95 ± 0.13 | 8.10 ± 0.38[a] |
| $b$ ($s^{-1}$) | 4.32 ± 0.09 | 4.19 ± 0.09[a] | 4.33 ± 0.11 | 4.37 ± 0.09[a] |
| $k_{tr}$ ($s^{-1}$) | 1.99 ± 0.05 | 1.83 ± 0.11[a] | 1.61 ± 0.10 | 1.57 ± 0.05[a] |

Maximal tension was measured by exposing muscle fibers to saturating $Ca^{2+}$ concentration (pCa 4.3) in a constantly stirred chamber. Tension cost was derived from the ATPase/tension relationship, as previously described (de Tombe and Stienen, 1995; Chandra et al., 2015). Parameters $c$ and $b$ were estimated by fitting the NLRD model to the force response phases to various amplitude stretch/release perturbations (Fig. 1; Ford et al., 2010). $c$ represents the rate of force decay to a minimum force point following a sudden stretch in ML, and $b$ represents the rate at which force rises at the new ML. $k_{tr}$ was estimated by fitting a monoexponential function to the rising phase of the force response to a large slack-restretch length maneuver and represents the rate of tension redevelopment (Brenner and Eisenberg, 1986). Estimates from several muscle fibers per group were averaged and presented as mean ± SEM. Statistical differences were analyzed using two-way ANOVA and subsequent post hoc multiple pairwise comparisons (Fisher's LSD method). The number of fibers measured (from three hearts) for all groups was 10.
[a]Not significantly different from $TnT_{WT}$ fibers.

was dissimilar at different SLs. When the interaction was not significant, we assessed the main effect of TnT at different SLs. To determine the source of significant interaction or main effect, post hoc $t$ tests using Fisher's least significant difference (LSD) method were analyzed. The criterion for statistical significance was set to $P < 0.05$. Data are presented as mean ± SEM.

### Online supplemental material

Details regarding expression and purification of recombinant guinea pig cardiac troponin subunits, preparation of guinea pig cardiac muscle fibers, Western blot analysis of reconstituted muscle fiber samples, composition of pCa solutions, NLRD model parameters, and measurement of $k_{tr}$ can be found in the Supplemental materials and methods. Western blot analysis of reconstituted muscle fibers (Fig. S1) and contractile dynamic data regarding the effect of $TnT_{F88L}$ at submaximal activation (Table S1) are also included.

## Results

### Western blot analysis of recombinant TnT incorporation in guinea pig cardiac muscle fibers

To assess the level of recombinant TnT incorporation, reconstituted $TnT_{WT}$ or $TnT_{F88L}$ muscle fibers were solubilized in 2.5% SDS solution and run on 8% SDS gel to separate endogenous and recombinant (*c-myc*–tagged) TnT, as described in Supplemental materials and methods. The inclusion of the *c-myc* tag at the N terminus allowed us to separate recombinant TnT ($TnT_{WT}$ or $TnT_{F88L}$) from the endogenous TnT via different migration on SDS gel. We and others have previously shown that the *c-myc* epitope at the N terminus of TnT does not affect cardiac function (Tardiff et al., 1998; Montgomery et al., 2001; Chandra et al., 2005). To quantify the level of incorporation of recombinant TnT (i.e., the amount of total endogenous TnT that was replaced by recombinant TnT) in reconstituted muscle fibers, we used Western blot analysis. Densitometric analysis of the band profiles from the Western blot revealed that the incorporation level of *c-myc*–tagged $TnT_{WT}$ was 77 ± 6%, and that of *c-myc*–tagged $TnT_{F88L}$ was 72 ± 7% (Fig. S1). Values reported as mean ± SD; $n = 3$.

### Effect of $TnT_{F88L}$ on $Ca^{2+}$-activated tension and $E_D$ at short and long SLs

To determine whether $TnT_{F88L}$ altered maximal tension and whether this effect varied in an SL-dependent manner, we assessed steady-state tension at maximal $Ca^{2+}$ activation at both short and long SLs. Two-way ANOVA did not show a significant TnT–SL interaction effect ($P = 0.28$) or a significant TnT main effect ($P = 0.66$) on maximal tension (Table 1). To corroborate our findings on maximal tension, we assessed $E_D$. Previous studies have shown that $E_D$ is strongly correlated to maximal tension and is therefore an index of the number of strongly bound XBs (Campbell et al., 2004; Ford et al., 2010). Similar to our findings on maximal tension, two-way ANOVA did not show a significant TnT–SL interaction effect ($P = 0.22$) or a significant TnT main effect ($P = 0.74$) on $E_D$. At short SL, $E_D$ was 639 $mN/mm^3$ for $TnT_{WT}$ fibers and 690 $mN/mm^3$ for $TnT_{F88L}$ fibers. At long SL, $E_D$ was 897 $mN/mm^3$ for $TnT_{WT}$ fibers and 867 $mN/mm^3$ for $TnT_{F88L}$ fibers. Observed changes in maximal tension and $E_D$ suggest that $TnT_{F88L}$ does not alter maximal activation.

Although $TnT_{F88L}$ did not alter maximal activation, we observed a substantial effect on tension at submaximal activations (pCa 5.6). At short SL, tension at pCa 5.6 was 4.59 $mN/mm^2$ for $TnT_{WT}$ fibers and 17.33 $mN/mm^2$ for $TnT_{F88L}$ fibers. At long SL, tension at pCa 5.6 was 14.02 $mN/mm^2$ for $TnT_{WT}$ fibers and 27.16 $mN/mm^2$ for $TnT_{F88L}$ fibers. Two-way ANOVA of tension at pCa 5.6 did not show a significant interaction effect ($P = 0.85$), but the main effect of TnT was significant ($P < 0.001$). $TnT_{F88L}$ increased tension at pCa 5.6 to a greater extent at short SL (278%, $P < 0.001$) than at long SL (93%; $P < 0.001$). Because of this greater increase in tension at short SL, the SL-dependent increase in tension at pCa 5.6 was ~3.6-fold less in $TnT_{F88L}$ fibers compared with $TnT_{WT}$ fibers. The SL-mediated increase in tension at pCa 5.6 was 207%

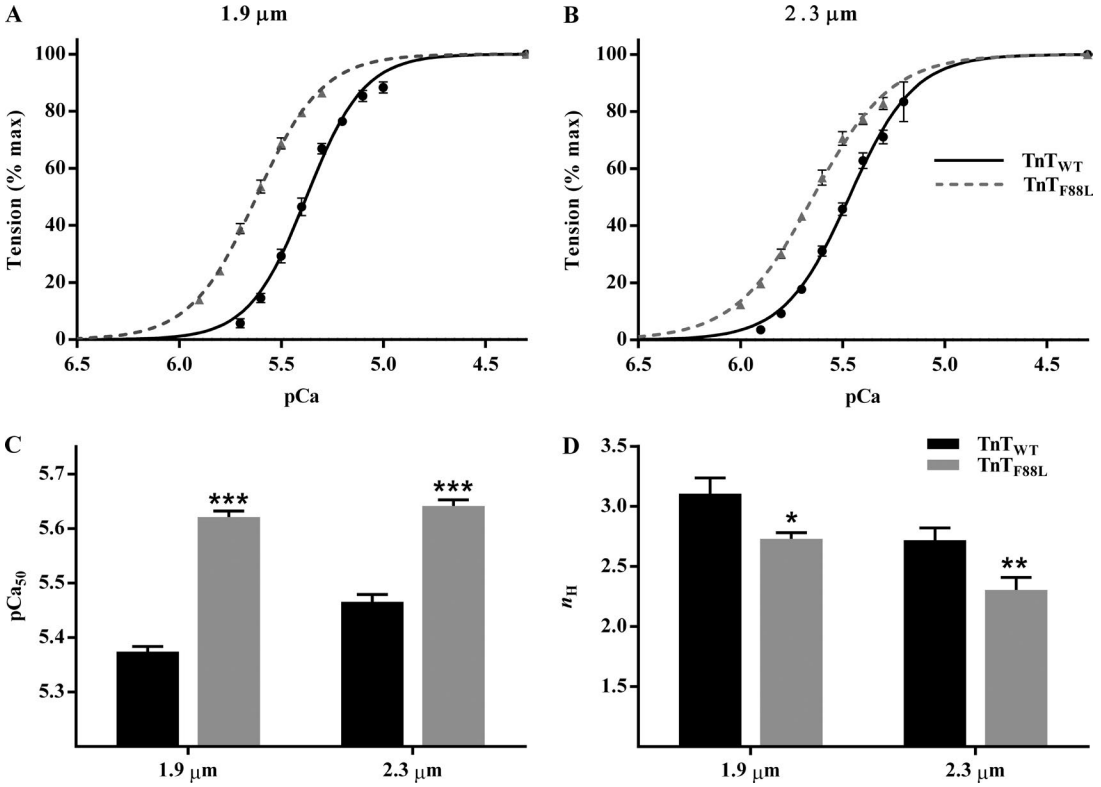


Figure 2. **Effect of TnT$_{F88L}$ on pCa–tension relationship at short and long SLs. (A and B)** A comparison of pCa–tension relationship between TnT$_{WT}$ and TnT$_{F88L}$ muscle fibers at short SL (A) and long SL (B). Steady-state tensions at various pCa values were normalized to the corresponding value at pCa 4.3 and plotted against pCa to derive pCa–tension data. Normalized pCa–tension data measured from several muscle fibers per group were averaged and presented as mean ± SEM. Error bars are smaller than symbols in some cases. **(C and D)** Bar graphs showing the effect of TnT$_{F88L}$ on myofilament $Ca^{2+}$ sensitivity (C; pCa$_{50}$) and cooperativity (D; $n_H$) at short and long SLs. Normalized pCa–tension data from each muscle fiber was individually fitted to Hill's model to derive pCa$_{50}$ and $n_H$. Estimates from several fibers per group were averaged and presented as mean ± SEM. Two-way ANOVA revealed a significant TnT–SL interaction effect (P = 0.003) on pCa$_{50}$. Two-way ANOVA did not show a significant TnT–SL interaction effect on $n_H$ (P = 0.84); however, the main effect of TnT was significant (P < 0.001). Post hoc multiple pairwise comparisons (Fisher's LSD) were used to determine significant differences between groups. Asterisks indicate significant difference from TnT$_{WT}$ at a given SL (*, P < 0.05; **, P < 0.01; ***, P < 0.001). The numbers of fibers measured (from three hearts) for TnT$_{WT}$ and TnT$_{F88L}$ at short SL were 10 and 10, and those at long SL were 9 and 10, respectively.

in TnT$_{WT}$ fibers (P < 0.001), whereas it was only 57% in TnT$_{F88L}$ fibers (P < 0.001). Our data on submaximal tension demonstrates that the SL-mediated increase in force is significantly attenuated by TnT$_{F88L}$, suggesting that TnT$_{F88L}$ may blunt ML-mediated increase in force production in heart muscle, which normally operates under submaximal activating conditions.

### Effect of TnT$_{F88L}$ on pCa$_{50}$ and $n_H$ at short and long SLs

A comparison of pCa–tension relationships shows a leftward shift in the pCa–tension relationship of TnT$_{F88L}$ muscle fibers at both short SL (Fig. 2 A) and long SL (Fig. 2 B). A cursory look indicates that the magnitude of leftward shift in pCa–tension relationship is greater at short than at long SL, suggesting that TnT$_{F88L}$ increases myofilament $Ca^{2+}$ sensitivity to a greater extent at short SL than at long SL. To quantify the magnitude of TnT$_{F88L}$-mediated effect on pCa–tension relationship, we used Hill model–derived parameters, pCa$_{50}$ and $n_H$. Two-way ANOVA revealed a significant TnT–SL interaction effect (P = 0.003) on pCa$_{50}$, suggesting that the effect of TnT$_{F88L}$ on pCa$_{50}$ is dissimilar at different SLs. Post hoc *t* tests indicated that TnT$_{F88L}$ significantly increased pCa$_{50}$ to a greater extent at short SL (0.25 units; P < 0.001; Fig. 2 C) than at long SL (0.17 units; P < 0.001; Fig. 2 C). This differential effect on pCa$_{50}$ impacted the SL dependence of pCa$_{50}$ in TnT$_{F88L}$ muscle fibers, such that pCa$_{50}$ was not different between short and long SL in TnT$_{F88L}$ muscle fibers. Although increasing SL from 1.9 to 2.3 μm significantly increased pCa$_{50}$ by 0.10 units in TnT$_{WT}$ fibers (P < 0.001; Fig. 2 C), it did not significantly increase pCa$_{50}$ in TnT$_{F88L}$ fibers (P = 0.22; Fig. 2 C), indicating that TnT$_{F88L}$ abolished the length-mediated increase in $Ca^{2+}$ sensitivity, a major mechanism underlying cardiac length-dependent activation. With regard to $n_H$, two-way ANOVA did not reveal a significant TnT–SL interaction effect on $n_H$ (P = 0.84); however, the main effect of TnT was significant (P < 0.001). Post hoc *t* tests revealed that TnT$_{F88L}$ attenuated $n_H$ at both short SL (12%; P = 0.011; Fig. 2 D) and long SL (15%; P = 0.005; Fig. 2 D), suggesting an impact on mechanisms governing myofilament cooperativity. This impact on myofilament cooperativity and abolishment of length-mediated increase in $Ca^{2+}$ sensitivity blunted the SL-mediated increase in tension at all $Ca^{2+}$ concentrations tested (Fig. 3).

### Effect of TnT$_{F88L}$ on the rate of XB detachment at short and long SLs

Previous studies have shown that mutations in TnT may alter the rate of XB detachment, *g* (Chandra et al., 2015; Gollapudi and

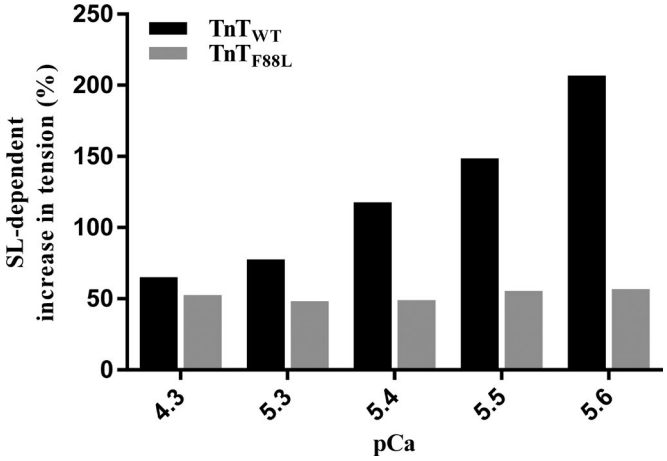


Figure 3. **Effect of TnT$_{F88L}$ on SL-dependent increase in tension.** Bar graph showing the percent increase in tension in response to an increase in SL from 1.9 to 2.3 µm in TnT$_{WT}$ (black) and TnT$_{F88L}$ (gray) fibers at various pCa values. For each pCa, steady-state tension values from muscle fibers per group were averaged, and percent difference between short and long SLs was calculated for TnT$_{WT}$ and TnT$_{F88L}$ groups. The minimum number of fibers measured (from three hearts) was nine per group.

Chandra, 2016a; Reda et al., 2016). Changes in SL have also been shown to impact *g* (Chandra et al., 2006; Stelzer and Moss, 2006; Ford and Chandra, 2013), such that an increase in SL decreases *g* and vice versa. To determine whether TnT$_{F88L}$ altered *g*, and whether such effect varied in an SL-dependent manner, we assessed estimates of *c* and tension cost. Previous studies have demonstrated a strong correlation between *c* and tension cost (Campbell et al., 2004; Gollapudi and Chandra, 2016b), and both provide an appropriate measure of XB detachment rate, *g*. *c* represents the rate of XB distortion dynamics after a sudden stretch in ML and is estimated by fitting the NLRD model to the family of force responses to various amplitude length perturbations. Two-way ANOVA of *c* did not show a significant TnT–SL interaction effect (P = 0.20) or a significant main effect of TnT (P = 0.32; Table 1). Our observations on *c* were corroborated by our estimates of tension cost. Two-way ANOVA of tension cost did not reveal a significant TnT–SL interaction effect (P = 0.13) or a significant main effect of TnT (P = 0.65; Table 1). Collectively, findings on *c* and tension cost strongly suggest that TnT$_{F88L}$ does not alter *g*.

### Effect of TnT$_{F88L}$ on XB turnover rate at short and long SLs

To determine whether TnT$_{F88L}$ altered the rate of XB turnover, and whether such effect varied in an SL-dependent manner, we assessed changes in two independent contractile parameters, *b* and $k_{tr}$. *b* represents the rate constant of delayed force rise after an increase in ML and is estimated by fitting the NLRD model to a family of force responses to various amplitude step-like ML perturbations (Ford et al., 2010); $k_{tr}$ represents the rate of force redevelopment after a large release–restretch length maneuver (Brenner and Eisenberg, 1986). Previous studies have shown that *b* and $k_{tr}$ are reliable measures of XB turnover rate (Campbell et al., 2004). Two-way ANOVA of *b* did not show a significant TnT–SL interaction effect (P = 0.37) or a significant main effect of TnT (P = 0.65; Table 1). Two-way ANOVA of $k_{tr}$ did not show a significant TnT–SL interaction effect (P = 0.49) or a significant main effect of TnT (P = 0.24; Table 1). Collectively, our observations suggest that TnT$_{F88L}$ does not alter XB turnover rate.

### Effect of TnT$_{F88L}$ on γ at short and long SLs

In our NLRD model, parameter γ represents the nonlinear interaction term, which is formulated as an effect by which the distortion of bound XBs influences the recruitment of other XBs. γ is estimated by fitting the NLRD model to a family of force responses to various amplitude length perturbations (Ford et al., 2010). From a physiological standpoint, γ is an indicator of the negative effect that strained XBs have on other force-bearing XBs. For example, when the negative impact of strained XBs on the state of other force-bearing XBs is less pronounced, the magnitude of force decline brought about by detachment of strained XBs is lesser (less prominent nadir), and thus γ is lower. Because such XB-based interactions are mediated by cooperative interactions within the thick and thin filaments, γ is thought to be influenced by allosteric/cooperative mechanisms in the myofilaments. A comparison of force responses to 2% sudden stretch shows that TnT$_{F88L}$ induces a less pronounced force decline at short SL but has no effect at long SL (Fig. 4, A and B). Two-way ANOVA of γ showed a marginally significant TnT–SL interaction effect on γ (P = 0.051), suggesting that TnT$_{F88L}$ altered γ differently at short and long SLs. Post hoc analysis showed that TnT$_{F88L}$ significantly decreased γ at short SL (16%; P = 0.015; Fig. 4 C); however, TnT$_{F88L}$ had no effect at long SL (P = 0.77; Fig. 4 C) when compared with TnT$_{WT}$. Differential effects on γ suggest that the TnT$_{F88L}$-mediated impact on thin filament–based allosteric/cooperative processes—which mediate XB-based cooperativity—is different at short and long SLs. Such differential effects attenuate the SL dependence of γ in TnT$_{F88L}$ fibers; this is demonstrated by the observation that when SL was increased from 1.9 to 2.3 µm, γ decreased by 36% (P < 0.001; Fig. 4 C) in TnT$_{WT}$ fibers but decreased by only 21% (P = 0.006; Fig. 4 C) in TnT$_{F88L}$ fibers, suggesting that SL-dependent effects on cooperative mechanisms that govern γ are attenuated by TnT$_{F88L}$. We also assessed γ at comparable levels of force generation in TnT$_{WT}$ and TnT$_{F88L}$ fibers during submaximal activations. Our data at submaximal activations corroborate our findings at maximal activation; TnT$_{F88L}$ significantly decreased γ only at short SL (Table S1).

### Effect of TnT$_{F88L}$ on the magnitude of ML-mediated XB recruitment at short and long SLs

To determine the TnT$_{F88L}$-mediated effect on the magnitude of ML-mediated XB recruitment, we assessed estimates of $E_R$ at maximal $Ca^{2+}$ activation (pCa 4.3). $E_R$ represents the magnitude of delayed force rise in response to an increase in ML, an effect that is mediated by XB-based cooperative mechanisms (Campbell et al., 2004; Campbell and Chandra, 2006; Stelzer et al., 2006). $E_R$ is estimated by fitting the NLRD model to a family of force responses to various amplitude length perturbations (Ford et al., 2010). Two-way ANOVA revealed a significant TnT–SL interaction effect on $E_R$ (P = 0.031), suggesting that the effect of TnT$_{F88L}$ on $E_R$ was different at short and long SLs. Post hoc analysis confirmed that TnT$_{F88L}$ increased $E_R$ by 39% at short SL (P = 0.043;

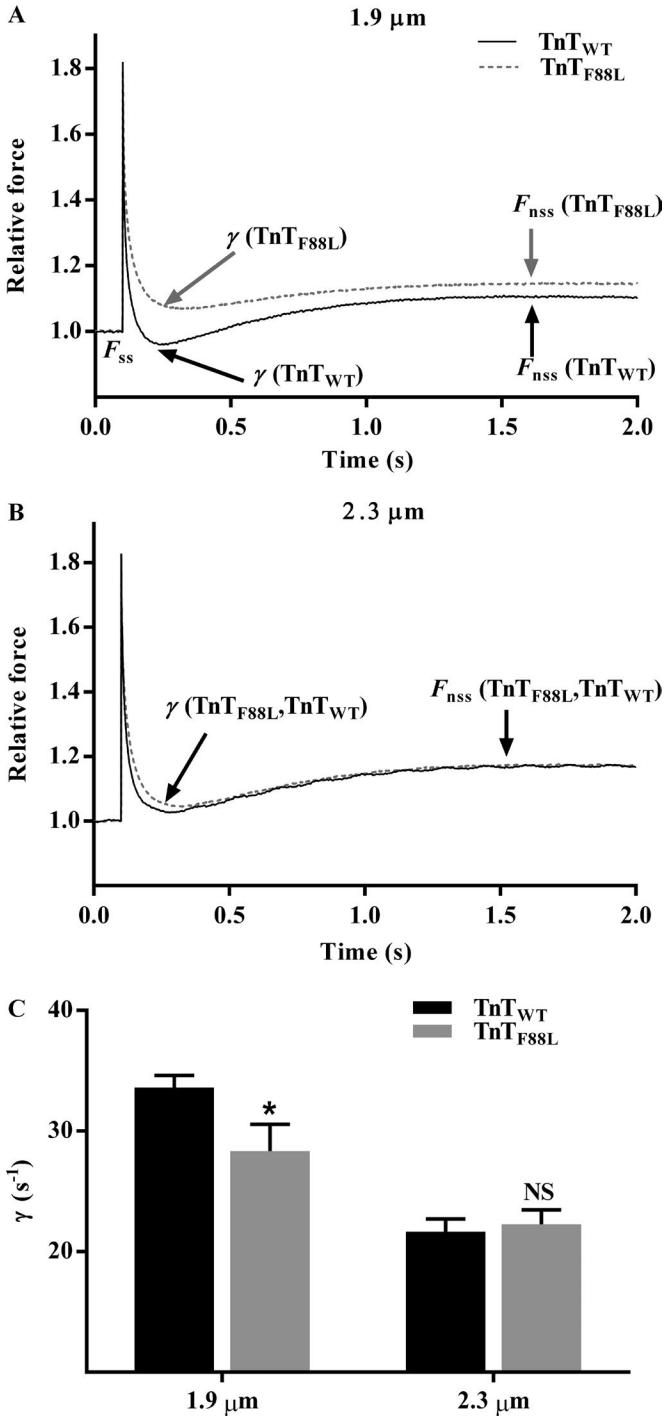


Figure 4. **Effect of TnT$_{F88L}$ on γ at short and long SLs. (A and B)** Effect of TnT$_{F88L}$ on the force response to a 2% sudden stretch imposed on a representative muscle fiber at short SL (A) and long SL (B). Force data were normalized to the isometric steady-state value before ML perturbation, and length data were normalized to the initial ML. $F_{ss}$ represents the isometric steady-state value before ML perturbation, and $F_{nss}$ represents the new steady-state force corresponding to an increase in ML. Parameter γ represents the negative impact of strained XBs on the recruitment of other force-bearing XBs and is estimated by fitting the NLRD model to the force response phases to various amplitude ML perturbations (Fig. 1; Ford et al., 2010). When the negative effect of strained XBs on the state of other force-bearing XBs is less pronounced, the magnitude of force decline is lesser; that is, the nadir is less pronounced and γ is attenuated. **(C)** Bar graph showing the effect of TnT$_{F88L}$ on γ at short and long SLs. Estimates from several muscle fibers per group were averaged and presented as mean ± SEM. Two-way ANOVA revealed a marginally significant TnT–SL interaction effect (P = 0.051) on γ. Post hoc multiple pairwise comparisons (Fisher's LSD) were used to determine significant differences between groups. Asterisks indicate significant difference from TnT$_{WT}$ at a given SL (*, P < 0.05). The number of fibers measured (from three hearts) for all groups was 10.

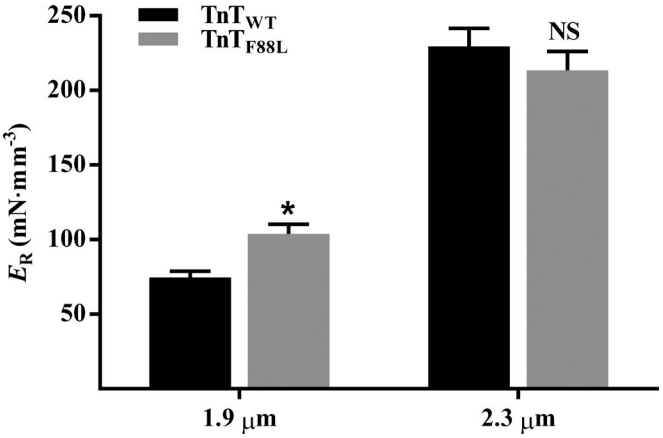


Figure 5. **Effect of TnT$_{F88L}$ on $E_R$ at short and long SLs.** $E_R$ corresponds to the ML-mediated increase in steady-state force and represents the magnitude of ML-mediated XB recruitment. $E_R$ is estimated as the slope of the linear relationship between ($F_{nss}$–$F_{ss}$) and ML changes, Δ$L$ (see Figs. 1 and 4, A and B). Estimates from several muscle fibers per group were averaged and presented as mean ± SEM. Two-way ANOVA revealed a significant TnT–SL interaction effect (P = 0.031) on $E_R$. Post hoc multiple pairwise comparisons (Fisher's LSD) were used to determine significant differences between groups. Asterisks indicate significant difference from TnT$_{WT}$ at a given SL (*, P < 0.05). The numbers of fibers measured (from three hearts) for TnT$_{WT}$ and TnT$_{F88L}$ at short SL were 9 and 10, and those at long SL were 10 and 10, respectively.

Fig. 5) but had no effect on $E_R$ at long SL (P = 0.25; Fig. 5), indicating that cooperative mechanisms governing $E_R$ were augmented at short SL. This dissimilar effect on $E_R$ at short and long SLs impacted the SL-mediated increase in $E_R$; for example, post hoc analysis showed that increasing SL increased $E_R$ by 207% (P < 0.001; Fig. 5) in TnT$_{WT}$ fibers, but by only 105% (P < 0.001; Fig. 5) in TnT$_{F88L}$ fibers. Such an observation suggests that TnT$_{F88L}$ attenuates SL-dependent effects on cooperative mechanisms underlying $E_R$. Here again, our data at submaximal activations corroborate our findings at maximal activation; TnT$_{F88L}$ significantly increased $E_R$ only at short SL (Table S1).

## Discussion

Data presented in this study provide novel insight regarding the effect of HCM-linked TnT$_{F88L}$ on contractile function and myofilament length-dependent activation. The major finding in our study is that the effect of TnT$_{F88L}$ mutation varies in an SL-dependent manner. Notably, TnT$_{F88L}$ increases pCa$_{50}$ to a greater extent at short SL than at long SL, such that pCa$_{50}$ is not different between short and long SLs in TnT$_{F88L}$ muscle fibers. That is, an increase in SL from 1.9 to 2.3 μm does not bring about the increase in pCa$_{50}$ that is typically associated with length-dependent activation of cardiac myofilaments, suggesting an impact on mechanisms governing cardiac length-dependent activation. Given that

length-dependent activation is a significant contributor to the Frank–Starling mechanism and that attenuated Frank–Starling mechanism is a hallmark of failing human hearts (Schwinger et al., 1994; van Dijk et al., 2012; Sequeira et al., 2013), our findings have important implications regarding cardiac dysfunction in patients harboring F87L.

Our observation that $TnT_{F88L}$ increases myofilament $Ca^{2+}$ sensitivity to a greater extent at short SL than at long SL raises two important questions: (1) how does $TnT_{F88L}$ augment thin filament $Ca^{2+}$ sensitivity, and (2) why is such an effect greater at short SL than at long SL? To address these questions, we must first consider mechanisms by which mutations in the CR of TnT may augment intrinsic thin filament responsiveness to $Ca^{2+}$. $TnT_{F88L}$ is located in the CR, a region of TnT involved in allosteric/cooperative interactions that regulate $Ca^{2+}$-mediated activation of thin filaments. Therefore, structural perturbations caused by mutations in the CR may affect processes regulating thin filament activation. In this regard, several lines of evidence show that mutations in the CR alter $Ca^{2+}$ sensitivity of Tn by modifying allosteric interactions within the thin filament (Liu et al., 2012; Sommese et al., 2013; Williams et al., 2016); for example, I79N and E163K mutations in TnT increase $Ca^{2+}$ affinity for Tn in reconstituted thin filament preparations containing actin:Tm:Tn (Sommese et al., 2013). However, I79N and E163K do not alter $Ca^{2+}$ affinity for Tn in in vitro preparations containing TnT + TnI + TnC, suggesting two important points: (1) mutation-mediated effect on thin filament $Ca^{2+}$ sensitivity is mediated by cooperative interactions within the thin filament, and (2) mechanisms other than a direct effect of the mutant on Tn $Ca^{2+}$ sensitivity may be involved in altering thin filament $Ca^{2+}$ sensitivity. Further support for this notion is provided by the observation that, although both R92L and R92W mutations in CR increase myofilament $Ca^{2+}$ sensitivity in muscle fibers (Ford et al., 2012), the rate of $Ca^{2+}$ dissociation from the isolated TnT + TnI + TnC complex is decreased by R92L but increased by R92W (Williams et al., 2016), suggesting that proper manifestation of the effect of CR mutations on myofilament $Ca^{2+}$ sensitivity requires participation of allosteric/cooperative processes within the thin filament.

Structural changes in the CR of TnT may alter thin filament $Ca^{2+}$ sensitivity by altering cooperative processes that affect the equilibrium between off/on states of regulatory unit (RU; Tn-Tm) located on actin filaments. CR not only promotes the binding of Tm to actin, but also aids in the assembly of Tm on the actin filament by promoting head-to-tail interactions between two contiguous Tms (Jackson et al., 1975; Heeley et al., 1987; Lehrer and Geeves, 1998; Palm et al., 2001). Therefore, CR plays a key role in mediating cooperative interactions between two neighboring RUs, which defines RU–RU cooperativity (Razumova et al., 2000). Thus, it is not surprising that mutations in CR modify RU–RU cooperativity by altering the coupling between CR and Tm (Palm et al., 2001; Hinkle and Tobacman, 2003). Because RU–RU cooperativity has the greatest effect on $n_H$ (Razumova et al., 2000), significant attenuation of $n_H$ is suggestive of a decrease in RU–RU cooperativity, which is expected to increase myofilament $Ca^{2+}$ sensitivity (Razumova et al., 2000). To elaborate, at lower levels of $Ca^{2+}$, when the majority of RUs are in the off state, cooperativity between two neighboring RUs tends to stabilize RUs in the off state. A consequence of this effect is that it requires more $Ca^{2+}$ to activate RUs, which results in decreased $Ca^{2+}$ sensitivity. When cooperative stabilization between neighboring RUs is decreased by $TnT_{F88L}$, it decreases the threshold for $Ca^{2+}$ to activate RUs, leading to increased $Ca^{2+}$ sensitivity of thin filaments. Such attenuation of RU–RU cooperativity may result from the weakening of TnT–Tm interactions (Gangadharan et al., 2017) and/or an effect on Tm–Tm overlap junction; in theory, this would lower the effective stiffness of the Tm chain and decrease cooperative communication between RUs. This line of reasoning is consistent with previous findings that have suggested that one primary mechanism by which HCM-linked thin filament mutations enhance myofilament $Ca^{2+}$ sensitivity is through attenuation of RU–RU cooperativity (Palm et al., 2001; Hinkle and Tobacman, 2003). Thus, a substantial increase in $Ca^{2+}$ sensitivity in $TnT_{F88L}$ fibers may be attributed to alterations in thin filament allosteric/cooperative mechanisms brought about by structural changes in RU.

Although the above explanation provides a molecular basis for the $TnT_{F88L}$-mediated effect on thin filament $Ca^{2+}$ sensitivity, it does not explain the differential effects observed at short and long SLs. Differential effects on tension at short and long SLs during submaximal activation may help explain the lack of SL-dependent effect on myofilament $Ca^{2+}$ sensitivity in $TnT_{F88L}$ fibers. Notably, at pCa 5.6, $TnT_{F88L}$ augments tension by 278% at short SL and by 93% at long SL, demonstrating that the ability of $TnT_{F88L}$ to increase the number of force-bearing XBs at submaximal activations is substantially greater at short SL. A consequence of such an increase in the number of strongly bound XBs at submaximal activation is that $TnT_{F88L}$ enhances XB-based cooperative mechanisms (XB–XB and XB–RU) more at short SL. Therefore, we posit that $TnT_{F88L}$ enhances XB-based cooperative feedback effect on thin filament to a greater degree at short SL. Because an increase in XB-based cooperativity is important for the SL-dependent increase in myofilament $Ca^{2+}$sensitivity (Allen and Kentish, 1985; Wang and Fuchs, 1994; Fitzsimons and Moss, 1998; Konhilas et al., 2002b; Smith et al., 2009), the lack of an increase in $Ca^{2+}$ sensitivity between short and long SL suggests that XB-based cooperative mechanisms are saturated at short SL in $TnT_{F88L}$ fibers. A consequence of proper manifestation of XB-based cooperativity is that the SL-mediated increase in tension (that is, an increase in tension associated with an increase in SL from 1.9 to 2.3 µm) is more pronounced at lower $Ca^{2+}$ concentrations (Campbell, 1997; Razumova et al., 2000). Indeed, the SL-dependent increase in tension in $TnT_{WT}$ fibers is more pronounced at lower $Ca^{2+}$ activations because the SL-dependent increase in XB-based cooperativity is normal in $TnT_{WT}$ fibers (Fig. 3). However, this SL-mediated increase in tension is absent in $TnT_{F88L}$ fibers at all $Ca^{2+}$concentrations tested, suggesting that XB-based cooperative mechanisms are saturated at short SL in $TnT_{F88L}$ fibers. To clarify, the $TnT_{F88L}$-mediated increase in XB-based cooperativity, combined with an increase in RU activation, causes a depletion in the number of RUs and XBs available for cooperative recruitment. Consequently, it limits the number of RUs and XBs that can be effectively engaged to enhance XB-based cooperative mechanisms as SL increases.

Additional evidence for increased XB-based cooperativity at short SL and disruption of SL-mediated effects on XB-based

cooperativity may be gleaned from our observations on two other contractile dynamic parameters, γ and $E_R$. Parameter γ represents thin filament–based regulatory mechanisms by which strained XBs negatively impact other force-bearing XBs (Ford et al., 2010). A significant decrease in γ at short SL in $TnT_{F88L}$ fibers suggests that the negative effect of strained XBs on force-bearing XBs is attenuated, a likely consequence of greater expression of XB-based cooperativity. We posit that increased XB-based cooperativity counteracts the negative impact of strained XBs on force-bearing XBs, leading to a decrease in γ at short SL. The augmenting effect of $TnT_{F88L}$ on XB-based cooperativity at short SL is also supported by the magnitude of ML-mediated XB recruitment, $E_R$, which is sensitive to changes in XB-based cooperativity (Campbell et al., 2004; Campbell and Chandra, 2006; Stelzer et al., 2006; Gollapudi et al., 2017). $TnT_{F88L}$ significantly increases $E_R$ at short SL (39%) but not at long SL, suggesting that $TnT_{F88L}$ imparts a greater effect on XB-based cooperativity at short SL. Just as it did in tension experiments, this saturation of XB-based cooperativity at short SL blunted the SL-mediated effects on γ (Fig. 4) and $E_R$ (Fig. 5) in $TnT_{F88L}$ fibers.

With respect to XB-based feedback effects (XB–XB and XB–RU cooperativity) and changes in $Ca^{2+}$ sensitivity, the consequence of augmented XB–RU cooperativity is of importance, because changes in XB–RU cooperativity are most prominently reflected by changes in $Ca^{2+}$ sensitivity (Razumova et al., 2000). In this context, a consequence of increased XB–RU cooperativity at short SL is that it engages more RUs in XB–RU population, causing the depletion of RU pool and limiting the scope of XB–RU population to increase as SL increases. Therefore, lack of SL-mediated increase in XB–RU cooperativity in $TnT_{F88L}$ fibers would explain why an increase in SL results in no further increase in myofilament $Ca^{2+}$ sensitivity (Fig. 2 C). Although we cannot definitively distinguish between the two types of XB-based cooperativity, findings from previous modeling simulations (Razumova et al., 2000)—in conjunction with data from our study—provide clues about the effect of $TnT_{F88L}$ on XB-based cooperativity. Previous modeling studies have suggested that changes in XB–XB cooperativity have an impact on maximal tension, $k_{tr}$, and $pCa_{50}$ such that an increase in XB–XB cooperativity augments maximal tension, slows $k_{tr}$, and decreases $pCa_{50}$ (and vice versa; Razumova et al., 2000). In this context, our observation that $TnT_{F88L}$ does not alter maximal tension and $k_{tr}$, and significantly increases $pCa_{50}$, allows us to speculate that $TnT_{F88L}$ may have little to no impact on XB–XB cooperativity.

### Conclusion

$TnT_{F88L}$ increases myofilament $Ca^{2+}$ sensitivity at both short and long SLs; however, the effect is disproportionately greater at short SL, which results in abolishment of length-dependent activation. Under submaximal activating conditions, increased myofilament $Ca^{2+}$ sensitivity, combined with an increase in $E_R$, may increase ventricular force output during systole and prolong systolic ejection time (Davis et al., 2001; Stelzer et al., 2006; Stelzer and Moss, 2006), leading to a delay in ventricular relaxation. Slowed ventricular relaxation would offer greater resistance to ventricular filling in late diastole such that ventricular diastolic pressure is elevated; this may lead to dyspnea, as observed in patients harboring F87L (Gimeno et al., 2009). Impairment of length-dependent activation suggests that the Frank–Starling mechanism may be significantly impaired in intact hearts containing F87L. Under increased hemodynamic demands, attenuation of the Frank–Starling mechanism may have severe consequences on heart function because it limits the ability of the heart to increase its stroke volume in response to an increase in venous return. In some cases, however, a substantial increase in myofilament $Ca^{2+}$ sensitivity and subsequent increase in myocardial force development may offer a benefit to F87L patients who are at advanced stages of heart failure. Patients at advanced stages of heart failure are likely to minimize high stress workloads and thus operate at lower end-diastolic volumes; under such conditions, increased force at short SL may improve contraction.

## Acknowledgments

This work was supported, in part, by the National Institutes of Health (HL-075643 to M. Chandra).

The authors declare no competing financial interests. This paper does not contain clinical studies of patient data.

Author contributions: S.M. Reda: study conception, design, data acquisition, data analysis, data interpretation, and drafting of the manuscript. M. Chandra: study conception, design, data interpretation, and drafting of the manuscript.

Henk L. Granzier served as editor.

Submitted: 12 December 2017
Revised: 9 March 2018
Accepted: 24 April 2018

## References

Abraham, D.M., R.T. Davis III, C.M. Warren, L. Mao, B.M. Wolska, R.J. Solaro, and H.A. Rockman. 2016. β-Arrestin mediates the Frank-Starling mechanism of cardiac contractility. *Proc. Natl. Acad. Sci. USA.* 113:14426–14431. https://doi.org/10.1073/pnas.1609308113

Allen, D.G., and J.C. Kentish. 1985. The cellular basis of the length-tension relation in cardiac muscle. *J. Mol. Cell. Cardiol.* 17:821–840. https://doi.org/10.1016/S0022-2828(85)80097-3

Arteaga, G.M., K.A. Palmiter, J.M. Leiden, and R.J. Solaro. 2000. Attenuation of length dependence of calcium activation in myofilaments of transgenic mouse hearts expressing slow skeletal troponin I. *J. Physiol.* 526:541–549. https://doi.org/10.1111/j.1469-7793.2000.t01-1-00541.x

Brenner, B., and E. Eisenberg. 1986. Rate of force generation in muscle: correlation with actomyosin ATPase activity in solution. *Proc. Natl. Acad. Sci. USA.* 83:3542–3546. https://doi.org/10.1073/pnas.83.10.3542

Campbell, K. 1997. Rate constant of muscle force redevelopment reflects cooperative activation as well as cross-bridge kinetics. *Biophys. J.* 72:254–262. https://doi.org/10.1016/S0006-3495(97)78664-8

Campbell, K.B., and M. Chandra. 2006. Functions of stretch activation in heart muscle. *J. Gen. Physiol.* 127:89–94. https://doi.org/10.1085/jgp.200509483

Campbell, K.B., M. Chandra, R.D. Kirkpatrick, B.K. Slinker, and W.C. Hunter. 2004. Interpreting cardiac muscle force-length dynamics using a novel functional model. *Am. J. Physiol. Heart Circ. Physiol.* 286:H1535–H1545. https://doi.org/10.1152/ajpheart.01029.2003

Chandra, M., J.J. Kim, and R.J. Solaro. 1999. An improved method for exchanging troponin subunits in detergent skinned rat cardiac fiber bundles. *Biochem. Biophys. Res. Commun.* 263:219–223. https://doi.org/10.1006/bbrc.1999.1341

Chandra, M., M.L. Tschirgi, and J.C. Tardiff. 2005. Increase in tension-dependent ATP consumption induced by cardiac troponin T mutation. *Am. J.*

*Physiol. Heart Circ. Physiol.* 289:H2112–H2119. https://doi.org/10.1152/ajpheart.00571.2005

Chandra, M., M.L. Tschirgi, I. Rajapakse, and K.B. Campbell. 2006. Troponin T modulates sarcomere length-dependent recruitment of cross-bridges in cardiac muscle. *Biophys. J.* 90:2867–2876. https://doi.org/10.1529/biophysj.105.076950

Chandra, V., S.K. Gollapudi, and M. Chandra. 2015. Rat cardiac troponin T mutation (F72L)-mediated impact on thin filament cooperativity is divergently modulated by α- and β-myosin heavy chain isoforms. *Am. J. Physiol. Heart Circ. Physiol.* 309:H1260–H1270. https://doi.org/10.1152/ajpheart.00519.2015

Davis, J.S., S. Hassanzadeh, S. Winitsky, H. Lin, C. Satorius, R. Vemuri, A.H. Aletras, H. Wen, and N.D. Epstein. 2001. The overall pattern of cardiac contraction depends on a spatial gradient of myosin regulatory light chain phosphorylation. *Cell.* 107:631–641. https://doi.org/10.1016/S0092-8674(01)00586-4

de Tombe, P.P., and G.J. Stienen. 1995. Protein kinase A does not alter economy of force maintenance in skinned rat cardiac trabeculae. *Circ. Res.* 76:734–741. https://doi.org/10.1161/01.RES.76.5.734

Fitzsimons, D.P., and R.L. Moss. 1998. Strong binding of myosin modulates length-dependent Ca2+ activation of rat ventricular myocytes. *Circ. Res.* 83:602–607. https://doi.org/10.1161/01.RES.83.6.602

Ford, S.J., and M. Chandra. 2013. Length-dependent effects on cardiac contractile dynamics are different in cardiac muscle containing α- or β-myosin heavy chain. *Arch. Biochem. Biophys.* 535:3–13. https://doi.org/10.1016/j.abb.2012.10.011

Ford, S.J., M. Chandra, R. Mamidi, W. Dong, and K.B. Campbell. 2010. Model representation of the nonlinear step response in cardiac muscle. *J. Gen. Physiol.* 136:159–177. https://doi.org/10.1085/jgp.201010467

Ford, S.J., R. Mamidi, J. Jimenez, J.C. Tardiff, and M. Chandra. 2012. Effects of R92 mutations in mouse cardiac troponin T are influenced by changes in myosin heavy chain isoform. *J. Mol. Cell. Cardiol.* 53:542–551. https://doi.org/10.1016/j.yjmcc.2012.07.018

Gangadharan, B., M.S. Sunitha, S. Mukherjee, R.R. Chowdhury, F. Haque, N. Sekar, R. Sowdhamini, J.A. Spudich, and J.A. Mercer. 2017. Molecular mechanisms and structural features of cardiomyopathy-causing troponin T mutants in the tropomyosin overlap region. *Proc. Natl. Acad. Sci. USA.* 114:11115–11120. https://doi.org/10.1073/pnas.1710354114

Gimeno, J.R., L. Monserrat, I. Pérez-Sánchez, F. Marín, L. Caballero, M. Hermida-Prieto, A. Castro, and M. Valdés. 2009. Hypertrophic cardiomyopathy. A study of the troponin-T gene in 127 Spanish families. *Rev. Esp. Cardiol.* 62:1473–1477. https://doi.org/10.1016/S0300-8932(09)73136-7

Gollapudi, S.K., and M. Chandra. 2016a. Dilated cardiomyopathy mutation (R134W) in mouse cardiac troponin T induces greater contractile deficits against α-myosin heavy chain than against β-myosin heavy chain. *Front. Physiol.* 7:443. https://doi.org/10.3389/fphys.2016.00443

Gollapudi, S.K., and M. Chandra. 2016b. The effect of cardiomyopathy mutation (R97L) in mouse cardiac troponin T on the muscle length-mediated recruitment of crossbridges is modified divergently by α- and β-myosin heavy chain. *Arch. Biochem. Biophys.* 601:105–112. https://doi.org/10.1016/j.abb.2016.01.008

Gollapudi, S.K., R. Mamidi, S.L. Mallampalli, and M. Chandra. 2012. The N-terminal extension of cardiac troponin T stabilizes the blocked state of cardiac thin filament. *Biophys. J.* 103:940–948. https://doi.org/10.1016/j.bpj.2012.07.035

Gollapudi, S.K., C.E. Gallon, and M. Chandra. 2013. The tropomyosin binding region of cardiac troponin T modulates crossbridge recruitment dynamics in rat cardiac muscle fibers. *J. Mol. Biol.* 425:1565–1581. https://doi.org/10.1016/j.jmb.2013.01.028

Gollapudi, S.K., J.C. Tardiff, and M. Chandra. 2015. The functional effect of dilated cardiomyopathy mutation (R144W) in mouse cardiac troponin T is differently affected by α- and β-myosin heavy chain isoforms. *Am. J. Physiol. Heart Circ. Physiol.* 308:H884–H893. https://doi.org/10.1152/ajpheart.00528.2014

Gollapudi, S.K., S.M. Reda, and M. Chandra. 2017. Omecamtiv mecarbil abolishes length-mediated increase in guinea pig cardiac myofiber $Ca^{2+}$ sensitivity. *Biophys. J.* 113:880–888. https://doi.org/10.1016/j.bpj.2017.07.002

Heeley, D.H., K. Golosinska, and L.B. Smillie. 1987. The effects of troponin T fragments T1 and T2 on the binding of nonpolymerizable tropomyosin to F-actin in the presence and absence of troponin I and troponin C. *J. Biol. Chem.* 262:9971–9978.

Hinkle, A., and L.S. Tobacman. 2003. Folding and function of the troponin tail domain. Effects of cardiomyopathic troponin T mutations. *J. Biol. Chem.* 278:506–513. https://doi.org/10.1074/jbc.M209194200

Holubarsch, C., T. Ruf, D.J. Goldstein, R.C. Ashton, W. Nickl, B. Pieske, K. Pioch, J. Lüdemann, S. Wiesner, G. Hasenfuss, et al. 1996. Existence of the Frank-Starling mechanism in the failing human heart. Investigations on the organ, tissue, and sarcomere levels. *Circulation.* 94:683–689. https://doi.org/10.1161/01.CIR.94.4.683

Jackson, P., G.W. Amphlett, and S.V. Perry. 1975. The primary structure of troponin T and the interaction with tropomyosin. *Biochem. J.* 151:85–97. https://doi.org/10.1042/bj1510085

Kobirumaki-Shimozawa, F., T. Inoue, S.A. Shintani, K. Oyama, T. Terui, S. Minamisawa, S. Ishiwata, and N. Fukuda. 2014. Cardiac thin filament regulation and the Frank-Starling mechanism. *J. Physiol. Sci.* 64:221–232. https://doi.org/10.1007/s12576-014-0314-y

Konhilas, J.P., T.C. Irving, and P.P. de Tombe. 2002a. Frank-Starling law of the heart and the cellular mechanisms of length-dependent activation. *Pflugers Arch.* 445:305–310. https://doi.org/10.1007/s00424-002-0902-1

Konhilas, J.P., T.C. Irving, and P.P. de Tombe. 2002b. Length-dependent activation in three striated muscle types of the rat. *J. Physiol.* 544:225–236. https://doi.org/10.1113/jphysiol.2002.024505

Korte, F.S., and K.S. McDonald. 2007. Sarcomere length dependence of rat skinned cardiac myocyte mechanical properties: dependence on myosin heavy chain. *J. Physiol.* 581:725–739. https://doi.org/10.1113/jphysiol.2007.128199

Lehrer, S.S., and M.A. Geeves. 1998. The muscle thin filament as a classical cooperative/allosteric regulatory system. *J. Mol. Biol.* 277:1081–1089. https://doi.org/10.1006/jmbi.1998.1654

Liu, B., S.B. Tikunova, K.P. Kline, J.K. Siddiqui, and J.P. Davis. 2012. Disease-related cardiac troponins alter thin filament Ca2+ association and dissociation rates. *PLoS One.* 7:e38259. https://doi.org/10.1371/journal.pone.0038259

Mamidi, R., S.L. Mallampalli, D.F. Wieczorek, and M. Chandra. 2013. Identification of two new regions in the N-terminus of cardiac troponin T that have divergent effects on cardiac contractile function. *J. Physiol.* 591:1217–1234. https://doi.org/10.1113/jphysiol.2012.243394

Montgomery, D.E., J.C. Tardiff, and M. Chandra. 2001. Cardiac troponin T mutations: correlation between the type of mutation and the nature of myofilament dysfunction in transgenic mice. *J. Physiol.* 536:583–592. https://doi.org/10.1111/j.1469-7793.2001.0583c.xd

Moss, R.L., and D.P. Fitzsimons. 2002. Frank-Starling relationship: long on importance, short on mechanism. *Circ. Res.* 90:11–13.

Narolska, N.A., S. Eiras, R.B. van Loon, N.M. Boontje, R. Zaremba, S.R. Spiegelen Berg, W. Stooker, M.A. Huybregts, F.C. Visser, J. van der Velden, and G.J. Stienen. 2005a. Myosin heavy chain composition and the economy of contraction in healthy and diseased human myocardium. *J. Muscle Res. Cell Motil.* 26:39–48. https://doi.org/10.1007/s10974-005-9005-x

Narolska, N.A., R.B. van Loon, N.M. Boontje, R. Zaremba, S.E. Penas, J. Russell, S.R. Spiegelenberg, M.A. Huybregts, F.C. Visser, J.W. de Jong, et al. 2005b. Myocardial contraction is 5-fold more economical in ventricular than in atrial human tissue. *Cardiovasc. Res.* 65:221–229. https://doi.org/10.1016/j.cardiores.2004.09.029

Nowak, G., J.R. Peña, D. Urboniene, D.L. Geenen, R.J. Solaro, and B.M. Wolska. 2007. Correlations between alterations in length-dependent Ca2+ activation of cardiac myofilaments and the end-systolic pressure-volume relation. *J. Muscle Res. Cell Motil.* 28:415–419. https://doi.org/10.1007/s10974-008-9136-y

Palm, T., S. Graboski, S.E. Hitchcock-DeGregori, and N.J. Greenfield. 2001. Disease-causing mutations in cardiac troponin T: identification of a critical tropomyosin-binding region. *Biophys. J.* 81:2827–2837. https://doi.org/10.1016/S0006-3495(01)75924-3

Plotnick, G.D., L.C. Becker, M.L. Fisher, G. Gerstenblith, D.G. Renlund, J.L. Fleg, M.L. Weisfeldt, and E.G. Lakatta. 1986. Use of the Frank-Starling mechanism during submaximal versus maximal upright exercise. *Am. J. Physiol.* 251:H1101–H1105.

Razumova, M.V., A.E. Bukatina, and K.B. Campbell. 2000. Different myofilament nearest-neighbor interactions have distinctive effects on contractile behavior. *Biophys. J.* 78:3120–3137. https://doi.org/10.1016/S0006-3495(00)76849-4

Reda, S.M., S.K. Gollapudi, and M. Chandra. 2016. L71F mutation in rat cardiac troponin T augments crossbridge recruitment and detachment dynamics against α-myosin heavy chain, but not against β-myosin heavy chain. *J. Muscle Res. Cell Motil.* 37:215–223. https://doi.org/10.1007/s10974-016-9460-6

Schwinger, R.H., M. Böhm, A. Koch, U. Schmidt, I. Morano, H.J. Eissner, P. Uberfuhr, B. Reichart, and E. Erdmann. 1994. The failing human heart is unable to use the Frank-Starling mechanism. *Circ. Res.* 74:959–969. https://doi.org/10.1161/01.RES.74.5.959

Sequeira, V., P.J. Wijnker, L.L. Nijenkamp, D.W. Kuster, A. Najafi, E.R. Witjas-Paalberends, J.A. Regan, N. Boontje, F.J. Ten Cate, T. Germans, et al. 2013. Perturbed length-dependent activation in human hypertrophic cardiomyopathy with missense sarcomeric gene mutations. *Circ. Res.* 112:1491–1505. https://doi.org/10.1161/CIRCRESAHA.111.300436

Smith, L., C. Tainter, M. Regnier, and D.A. Martyn. 2009. Cooperative cross-bridge activation of thin filaments contributes to the Frank-Starling mechanism in cardiac muscle. *Biophys. J.* 96:3692–3702. https://doi.org/10.1016/j.bpj.2009.02.018

Sommese, R.F., S. Nag, S. Sutton, S.M. Miller, J.A. Spudich, and K.M. Ruppel. 2013. Effects of troponin T cardiomyopathy mutations on the calcium sensitivity of the regulated thin filament and the actomyosin cross-bridge kinetics of human β-cardiac myosin. *PLoS One.* 8:e83403. https://doi.org/10.1371/journal.pone.0083403

Stelzer, J.E., and R.L. Moss. 2006. Contributions of stretch activation to length-dependent contraction in murine myocardium. *J. Gen. Physiol.* 128:461–471. https://doi.org/10.1085/jgp.200609634

Stelzer, J.E., L. Larsson, D.P. Fitzsimons, and R.L. Moss. 2006. Activation dependence of stretch activation in mouse skinned myocardium: implications for ventricular function. *J. Gen. Physiol.* 127:95–107. https://doi.org/10.1085/jgp.200509432

Stienen, G.J., R. Zaremba, and G. Elzinga. 1995. ATP utilization for calcium uptake and force production in skinned muscle fibres of Xenopus laevis. *J. Physiol.* 482:109–122. https://doi.org/10.1113/jphysiol.1995.sp020503

Tardiff, J.C., S.M. Factor, B.D. Tompkins, T.E. Hewett, B.M. Palmer, R.L. Moore, S. Schwartz, J. Robbins, and L.A. Leinwand. 1998. A truncated cardiac troponin T molecule in transgenic mice suggests multiple cellular mechanisms for familial hypertrophic cardiomyopathy. *J. Clin. Invest.* 101:2800–2811. https://doi.org/10.1172/JCI2389

van der Velden, J., A.F. Moorman, and G.J. Stienen. 1998. Age-dependent changes in myosin composition correlate with enhanced economy of contraction in guinea-pig hearts. *J. Physiol.* 507:497–510. https://doi.org/10.1111/j.1469-7793.1998.497bt.x

van Dijk, S.J., E.R. Paalberends, A. Najafi, M. Michels, S. Sadayappan, L. Carrier, N.M. Boontje, D.W. Kuster, M. van Slegtenhorst, D. Dooijes, et al. 2012. Contractile dysfunction irrespective of the mutant protein in human hypertrophic cardiomyopathy with normal systolic function. *Circ Heart Fail.* 5:36–46. https://doi.org/10.1161/CIRCHEARTFAILURE.111.963702

Wang, Y.P., and F. Fuchs. 1994. Length, force, and Ca(2+)-troponin C affinity in cardiac and slow skeletal muscle. *Am. J. Physiol.* 266:C1077–C1082. https://doi.org/10.1152/ajpcell.1994.266.4.C1077

Williams, M.R., S.J. Lehman, J.C. Tardiff, and S.D. Schwartz. 2016. Atomic resolution probe for allostery in the regulatory thin filament. *Proc. Natl. Acad. Sci. USA.* 113:3257–3262. https://doi.org/10.1073/pnas.1519541113